eman ta zabal zazu
Universidad del País Vasco
Euskal Herriko Unibertsitatea
ZIENTZIA ETA TEKNOLOGIA FAKULTATEA
FACULTAD DE CIENCIA Y TECNOLOGÍA

Degree Final Project / Gradu Amaierako Lana / Trabajo Fin de Grado

Degree in Biochemistry and Molecular Biology / Biokimika eta Biologia Molekularreko gradua / Grado en Bioquímica y Biología Molecular

In vivo multimodal imaging of adenosine A_2A receptors after experimental stroke

Author/Egilea/Autora:

Maider Garbizu Albisu

Director/Zuzendaria/Director:

Abraham Martín Múñoz

Co-director/Zuzendarikidea/Codirectora:

Ana Zubiaga Elordieta

Leioa, 18th June 2021/ Leioa, 2021eko ekainaren 18a / Leioa, 18 de junio de 2021

INDEX

Introduction

Stroke is one of the most common pathologies worldwide, being the second leading cause of death and the third leading cause of disability in western countries (Feigin et al., 2017). It is a medical condition characterised by the death of brain cells as a result of the lack of oxygen and glucose due to the blood flow interruption to the brain by the rupture or the blockage of a brain blood vessel. The type of stroke caused by the rupture of an artery is called haemorrhagic stroke, whereas the one caused by the blockage of a vessel is known as ischemic stroke (Grysiewicz et al., 2008).

Ischemic stroke is an acute cerebrovascular disease characterised by a cascade of pathological events including excitotoxicity, inflammation and cellular death. In fact, due to the lack of oxygen, brain cells lose their potential to produce energy and as ATP-dependent ion channels fail, the depolarisation of the cell membrane occurs. As a consequence, voltage-dependent Ca^{2+} channels are activated and Ca^{2+} enters to the cell, which triggers extra liberation of glutamate. Glutamate is an excitatory neurotransmitter and, therefore, its high concentration produces excitatory effects in both neural and glial cells. Subsequently, brain cells release Ca^{2+} dependent enzymes such as proteases and phospholipases, as well as reactive oxygen species (ROS), which are detrimental and contribute to the oedema formation, inflammation and cell death (Broughton et al., 2009; Martín et al., 2018; Belov-Kirdajova et al., 2020). Nevertheless, the region affected by ischemic stroke is not homogenously affected regarding metabolic and ionic changes and, therefore, two different regions can be distinguished within the infarcted area: the core and the penumbra. The core is characterised by permanent and lethally depolarisations of cells, while the penumbra is characterised by repetitive depolarisations known as peri-infarct depolarisations (Dirnagl et al., 1999).

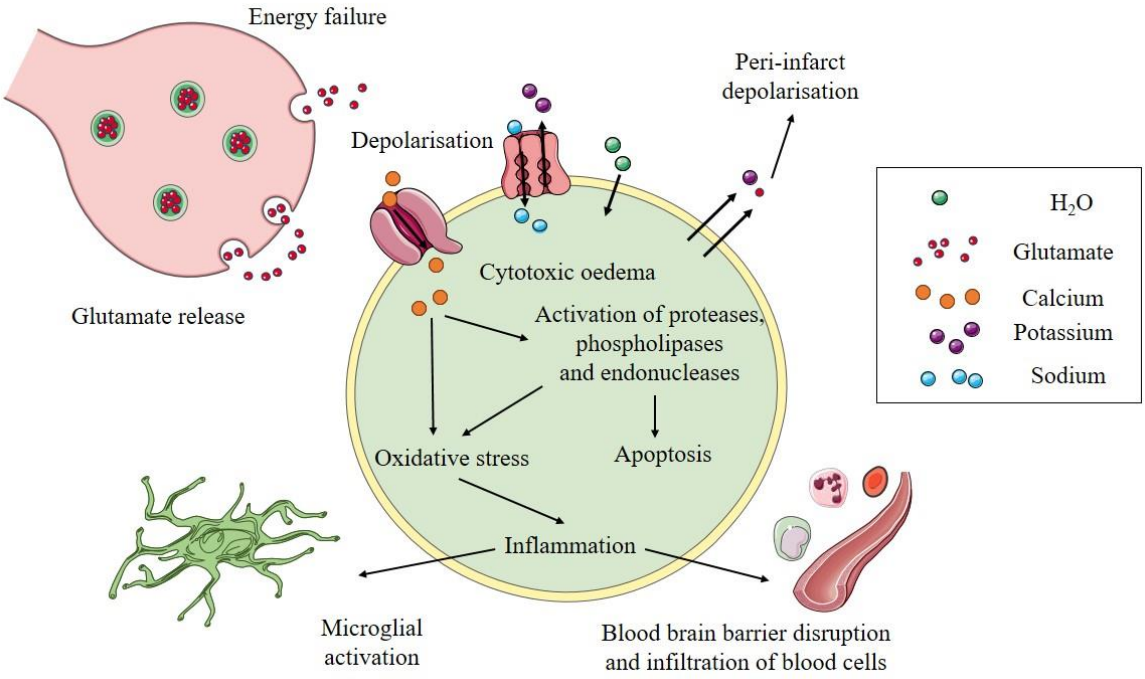

Figure 1. Simplified overview of the ischemic cascade. Neurons depolarise due to the energy failure**.** Glutamate receptors are activated and Ca^{2+} enters to the cell. Similarly, Na^{+} also enters to the cell, while K^{+} is released. Diffusion of K^{+} and glutamate to the

extracellular compartment can trigger to peri-infarct polarisation. H_2O enters to the cell because of osmotic gradients and leads to oedema. The intracellular Ca^{2+} activates different enzymes and produces oxidative stress (free radicals). Free radicals trigger the formation of inflammatory mediators, which activate microglia and lead to the infiltration of blood cells.

Ischemic stroke leads to an increase of the concentrations of purines, including adenosine 5'-triphospate (ATP) and adenosine. These biomolecules act as extracellular signalling molecules through a wide variety of metabotropic P1, metabotropic P_2Y and ionotropic P_2X purinergic receptors (Burnstock, 2007). Particularly, P1 receptors are specific for adenosine and there are four different subtypes (A_1, A_2A, A_2B, and A_3), which are G protein-coupled receptors (GPCR) with seven transmembrane domains (Fredholm et al., 2001). The expression of adenosine receptors (ARs) is widely distributed throughout the whole body including tissues such as heart, blood cells, kidney or brain, which implies many chemical effects (Borea et al., 2018). Therefore, adenosine has been related to many different physiological processes within the central nervous system (CNS), such as sleep homeostasis (Peng et al., 2020). However, the affinity of each receptor for adenosine is different and while A_1 and A_2A receptors show a high affinity, A_2B and A_3 receptors need higher concentrations of adenosine to be activated (Dunwiddie & Masino, 2001).

For this reason, adenosine and its receptors might be promising imaging biomarkers for diagnosis and therapy evaluation of cerebrovascular diseases such as stroke. Particularly, the longitudinal expression of A_1 adenosine receptors (A_1ARs) after cerebral ischemia has recently been studied using PET (Joya et al., 2021). This study observed that the [^{18}F]CPFPX-PET signal increased at days 3 and 7 in relation to day 1 after stroke, concluding that it could be a promising imaging biomarker for ischemic stroke. Besides, A_1ARs showed a neuroprotective role against cerebral ischemia trough the reduction of both reactive and proliferative microglia/macrophages.

Conversely, the longitudinal expression of adenosine A_2A receptors (A_2ARs) after ischemic stroke has not been described yet and *in vivo* imaging techniques may be helpful to evaluate their *in vivo* expression. Non-invasive positron emission tomography (PET) is one of those *in vivo* imaging modalities used to diagnose neurological diseases such as stroke. It is based on the administration of labelled molecules with a positron emitting isotope called radiotracer which binds to enzymes and receptors, among others (Janssen et al., 2016). Progress in radiotracer chemistry has allowed for the development of new compounds to study ARs *in vivo*, either agonists or antagonists. One of those radiotracers is [^{11}C]SCH442416, an antagonist compound with a high affinity for A_2ARs (Ki=0.5), which is one of the most selective compounds when compared to other established radiotracers for A_2ARs (Bauer & Ishiwata, 2009). In addition, it has been shown that [^{11}C]SCH442416 can be used not only in rodents, but also in monkeys (Moresco et al., 2005) and humans (Ramlackansingh et al., 2011).

As it is previously mentioned, *in vivo* imaging techniques have demonstrated that A_1ARs are interesting imaging biomarkers of ischemia, since adenosine is a mediator in the ischemic response. However, the *in vivo* distribution of other ARs including A_2ARs has been scarcely explored followed cerebral ischemia.

Hypothesis and objective

We hypothesise that A_2ARs have a key role in the ischemic response. For that reason, the main objective of this study was to evaluate the *in vivo* distribution of A_2ARs before and after cerebral ischemia. To that end, rats were analysed with PET imaging and magnetic resonance imaging (MRI) during the following month after a preclinical model of ischemic stroke.

Materials and methods

The experimental protocol of cerebral ischemia in rats and the acquisition of both PET and MRI-T_2W images were conducted at CIC biomaGUNE by the group of Abraham Martín. However, the analysis of the images obtained were conducted at Achucarro – Basque Center for Neuroscience by the author of this work.

Cerebral ischemia

Six adult male Sprague-Dawley rats (Janvier, France) were used for the experiment. Animals were anesthetised and induced to ischemic conditions by a transitory middle cerebral artery occlusion (MCAO) for 90 minutes. The experimental protocol was conducted as previously reported by Joya and colleagues (Joya et al., 2021), following the ARRIVE guidelines and Directives of the European Union on animal ethics and welfare. In brief, animals were anesthetised with 2.5% isoflurane in 100% O_2 and a 2.6 cm length of 4-0 monofilament nylon suture was introduced into the right external carotid artery up to the level of the origin of the MCA was reached. During occlusion, animals were placed in their cages with free access to food and water. 10 minutes before the end of 90-min occlusion, rats were re-anesthetised, the filament was removed to allow reperfusion and animals were kept in their cages. The study was approved by the animal ethics committee of CIC biomaGUNE.

Experimental set up

Rats were subjected to T_2-weighted (T_2W) MRI scans 24 h after reperfusion (i) to include animals showing cerebral ischemia in PET studies and (ii) to measure the volume of infarction. Rats were repeatedly subjected to PET scanning at day 0 (before MCAO) and at days 1, 3, 7, 14, 21 and 28 after cerebral ischemia to describe the distribution of A_2ARs in the rat brain.

Magnetic resonance imaging

Rats were anesthetised with isoflurane (2-2.5%) in a 30/70% mixture of O_2/N_2 to obtain MRI-T_2W images. Rats were put on a rat compatible MRI holder with normothermic conditions. Animal respiration rate and temperature were constantly assessed by a SAIIM1030 system (SA Instruments, NY, USA) while rats were in the MRI magnet. MRI images were acquired with a 7T horizontal bore Bruker Biospec USR 70/30 MRI system (Bruker Biospin GmbH, Ettlingen, Germany), interfaced to an AVANCE III console and with a BGA12-S imaging gradient insert (with a maximal gradient strength of 400 mT/m, switchable within 80µs). Measurements were performed with a 72 mm volumetric quadrature coil for excitation and a 20 mm rat brain

surface coil for reception. In order to focus on the regions of interest (ROIs), a scout scan was acquired at the beginning of the imaging session. MRI-T_2W images were obtained with a Bruker's RARE (Rapid Acquisition Relaxation Enhancement) sequence (Effective TE = 40 ms, TR 4400 ms, NA = 2; Matrix = 256 x 256 points; FOV = 25.6 x 25.6 mm; spatial resolution = 100 x 100 µm; 24 slices of 1 mm thickness covering the whole brain) to assess the volume of the infarcted area.

Magnetic resonance imaging analysis

For image analysis, the open source software imageJ (National Institutes of Health, Maryland, USA) was used to define ROIs manually. Different regions were analysed including the total volume of ipsilateral and contralateral cerebral hemispheres, striatum and cortex. Moreover, the total volume of infarction was also evaluated, as well as the infarcted area in both the striatum and cortex. The total volume of the regions mentioned was quantified by summing the areas of slices based on hyperintense signals.

Radiochemistry

The radiotracer used was [^{11}C]SCH442416, a selective and brain-penetrant antagonist of A_2ARs. The labelled molecule was generated in an IBA Cyclone 18/9 cyclotron and transferred to a TRACERlab FXC Pro synthesis module (GE Healthcare, Waukesha, WI, USA). The synthesis and quality control were conducted following previous protocols described by Moresco and colleagues (Moresco et al., 2005).

Positron emission tomography scans and data acquisition

PET images were acquired using an Explore Vista PET-CT camera (GE Healthcare, Waukesha, WI, USA). Rats were anesthetised with 2-2.5% of isoflurance in 100% O_2 and were placed into a PET acquisition system rat compatible holder. Rats were maintained in normothermia and their respiration rate and temperature were continuously assessed while the acquisition of images using a SAII M1030 system (SA Instruments, NY, USA). The radiotracer was administered intravenously by the tail vein using a 24-gauge catheter. Animals were scanned longitudinally before and during the following month after cerebral ischemia. The PET images obtained were acquired dynamically during 60 minutes using 36 frames (2 x 5s, 4 x 10s, 5 x 20s, 5 x 30s, 5 x 60s, 5 x 120s, 5 x 180s, 5 x 300s).

Positron emission tomography image analysis

An image analysis software called PMOD (version 3.5, PMOD Technologies Ltd, Zurich, Switzerland) was used to analyse PET signal. PET images were manually co-registered to MRI brain template to obtain spatial normalisation. Two different types of volumes of interest (VOIs) were defined: (1) A first set of VOIs was established to assess the whole brain [^{11}C]SCH442416-PET signal. Those VOIs were manually drawn in both the ipsilateral and contralateral hemispheres on slices of MRI-T_2W rat brain template from PMOD software. (2) Another set of VOIs was automatically defined in the striatum, hypothalamus, thalamus, cortex, hippocampus, and cerebellum by using the regions proposed by PMOD rat brain template, to assess the evolution of [^{11}C]SCH442416-PET signal in both ipsilateral and contralateral hemispheres. The last four

frames were used to quantify radiotracer uptake during the last 15 minutes. Average values were calculated as percentage of injected dose per cubic centimetre (%ID/cc).

Simplified Reference Tissue Model

Simplified Reference Tissue Model (SRTM) is a kinetic model to quantify the kinetic parameters of a receptor in PET studies without the need to measure the arterial input function. Particularly, this model considers that there is a brain region without specific binding of the radiotracer, which is known as reference tissue. The model is based on the following assumptions: (1) the volume of distribution of unspecific binding is the same in both the reference and target tissues; (2) the pathology under study does not affect the reference tissue; (3) the kinetic parameters of the target tissue can be defined by a single compartment. The most important parameter of this model is the non-displaceable binding potential (BPnd), which refers to the ratio of precisely bound radiotracer to that of non-displaceable radiotracer in tissue at equilibrium. Other parameters such as R_1 and k_2a are also obtained by this model, defining the relative influx of radioactivity and the outflow rate constant from specific region to plasma (Lammertsma & Hume, 1996). The reference tissue used in this study was the cerebellum, because the expression of A_2ARs is almost negligible in that region of the brain (Rosin et al., 1998). Hence, [^{11}C]SCH442416 has been described as one of the most selective radiotracers for A_2ARs based on the uptake ratio of striatum (receptor-rich region) to cerebellum (receptor-poor region) (Bauer & Ishiwata, 2009).

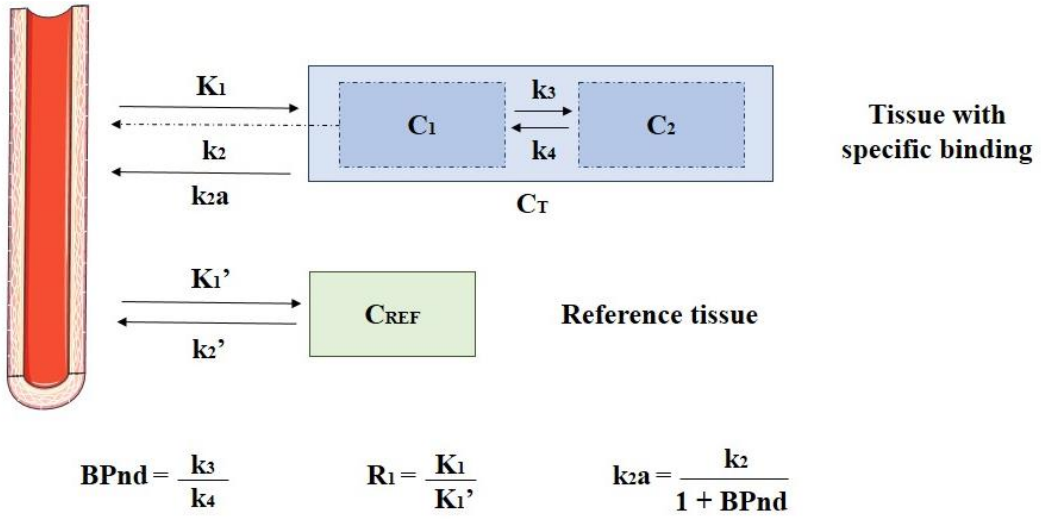

Figure 2. Simplified Reference Tissue Model (SRTM). It is a model to assess the quantification of receptor kinetics without assessing the arterial input function. C_{REF}= concentration in reference tissue; C_1= concentration of free radiotracer; C_2= concentration of specifically bound radiotracer; C_T= sum of C_1 and C_2; K_1= the rate constant to transfer from plasma to free region; k_2= the rate constant to transfer from free to plasma; k_3= the rate constant to transfer from free to bound region; k_4= the rate constant to transfer from bound to free region; k_2a= the overall rate constant to transfer from specific region to plasma; K_1'= the rate constant to transfer from plasma to reference region; k_2'= the rate constant to transfer from reference region to plasma; BPnd= the ratio of specific to non-displaceable binding; R_1= ratio of radiotracer entering the tissue with specific binding relative to reference tissue.

Statistical analyses

Statistical analyses were calculated using GraphPad Prism 8 (GraphPad Software LLC, San Diego, USA). The percentage of injected dose per cubic centimetre (%ID/cc), BPnd, influx (R_1) and efflux (k_2a) values in each region at different time point after ischemic stroke were averaged and compared using repeated measures ANOVA followed by Bonferrani multiple-comparison tests (post-hoc analysis). Similarly, the volumes of infarction within the hemisphere, cortex and striatum were also averaged and compared using repeated measures ANOVA followed by Bonferroni test for post-hoc analysis. Additionally, the correlation between infarcted ipsilateral hemisphere and midline displacement was performed with linear regression. The level of significance was set at $P < 0.05$.

Results

PET imaging evaluation of A_2ARs in the healthy brain

The expression of A_2ARs in healthy rat brains (control) was evaluated by PET. Time-activity curves (TACs) were quantified in different brain regions (striatum, hypothalamus, thalamus, cortex, hippocampus and cerebellum) to assess the concentration (%ID/cc) of [^{11}C]SCH442416-PET signal uptake. The radiotracer showed a fast uptake in the different brain regions studied followed by a wash-up until reached steady state during the last 15 minutes. Likewise, the highest %ID/cc value was observed in the striatum in relation to the other brain regions (Fig. 3A-C). Despite this, cerebral regions such as hypothalamus, thalamus, cortex, hippocampus and cerebellum showed high [^{11}C]SCH442416 uptake taking into account the low signal showed by PET images in these brain areas (Fig. 3B). For this reason, a more concise quantification of PET data was carried out with SRTM to discard the existence of non-specific binding by some of the rat brain regions.

Kinetic parameters including BPnd, R_1 and k_2a were analysed with SRTM using the cerebellum as the reference tissue region. These results showed a significant increase of BPnd in the striatum in comparison to other rat brain regions ($p < 0{,}001$), which showed almost negligible values. As is it previously mentioned, BPnd refers to the ratio of bound to free radiotracer in a specific region in the brain. Therefore, these results supported the existence of non-specific [^{11}C]SCH442416 binding in hypothalamus, thalamus, cortex and hippocampus. In contrast, no significant differences of the influx of the radiotracer to a specific region of the brain (R_1) and the efflux of the radiotracer from a specific region to the blood compartment (k_2a) were observed among different regions (Fig. 3D to F).

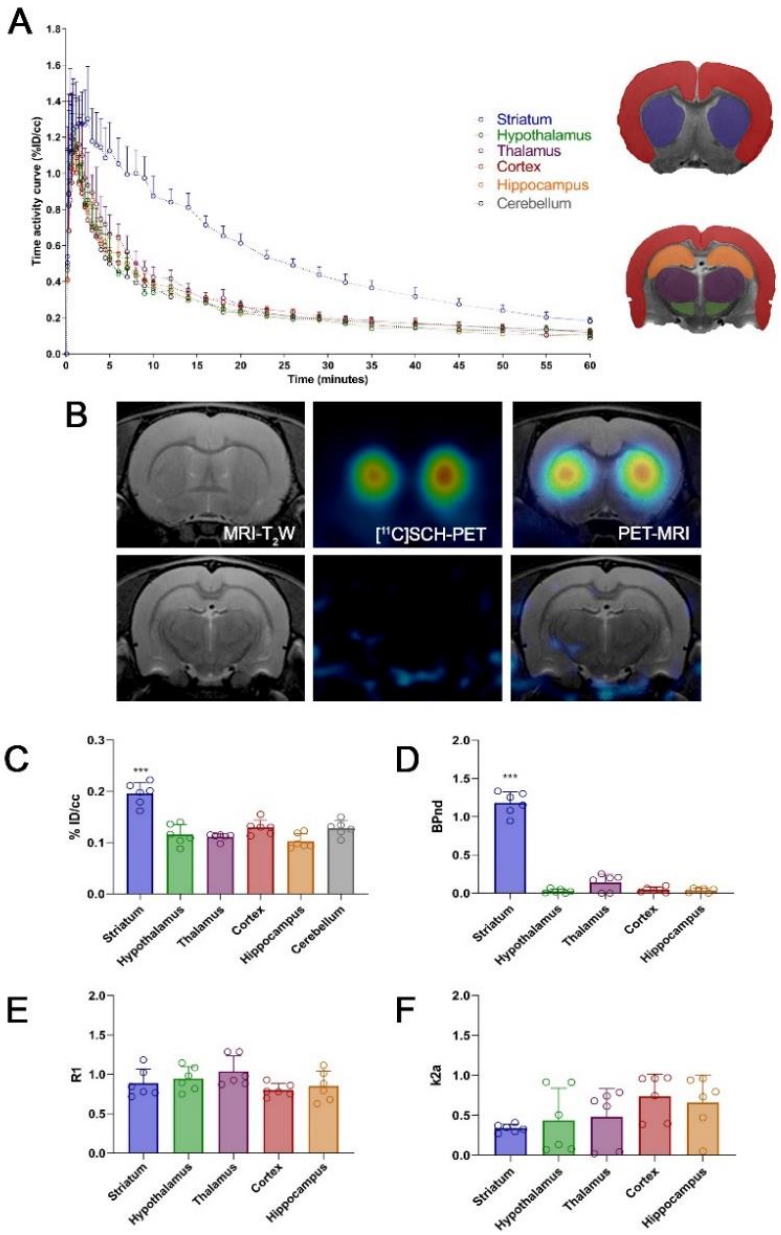

Figure 3. Expression of A_2ARs in healthy rat brains. A: Time activity curve (%ID/cc) of [^{11}C]SCH442416 in each rat brain region. B: MRI-T_2W, [^{11}C]SCH442416-PET and co-registered MRI-PET images in healthy conditions (different axial planes in accordance to the regions studied). C: %ID/cc in different regions of the brain. D to F: Kinetic parameters of BPnd (D), R_1 (E), and k_2a (F) obtained in different regions using SRTM.

Evaluation of brain infarction with MRI

MRI-T_2W images of axial planes at day 1 are shown in the figure 4A. Hyperintense regions of the images demonstrated the vasogenic oedema formation due to the ischemic stroke.

The extent of brain lesion was assessed at 24 hours after reperfusion showing a total volume of infarction of 282.78 ± 121.82 mm^3 (mean ± sd). The most affected areas by the ischemic stroke were the cortex and striatum, since almost all the animals showed corticostrial infarctions. The volume of infarction in the cortex was 198.28 ± 98.67 mm^3, whereas the striatum volume was 47.99 ± 8.68 mm^3. As a result, more than

80% of infarction was distributed in the cortex and striatum and the rest was distributed in other brain regions such as hippocampus (data non shown) (Fig. 4B-C).

The percentage of infarcted volume within each region (including the hemisphere, cortex and striatum) was also analysed. These results showed that in contrast to the percentage infarcted within the hemisphere (35%), most of the area of both the cortex (74%) ($p < 0.001$) and striatum was infarcted (69%) ($p < 0.01$) (Fig. 4D). Moreover, linear regression was performed to study the relationship between the volume of infarcted ipsilateral hemisphere (%) and midline displacement (%). Indeed, these results showed a significant correlation between the volume of infarction and the midline displacement at 24 hours after cerebral ischemia ($r^2 = 0.9718$, $p < 0.001$) (Fig. 4E).

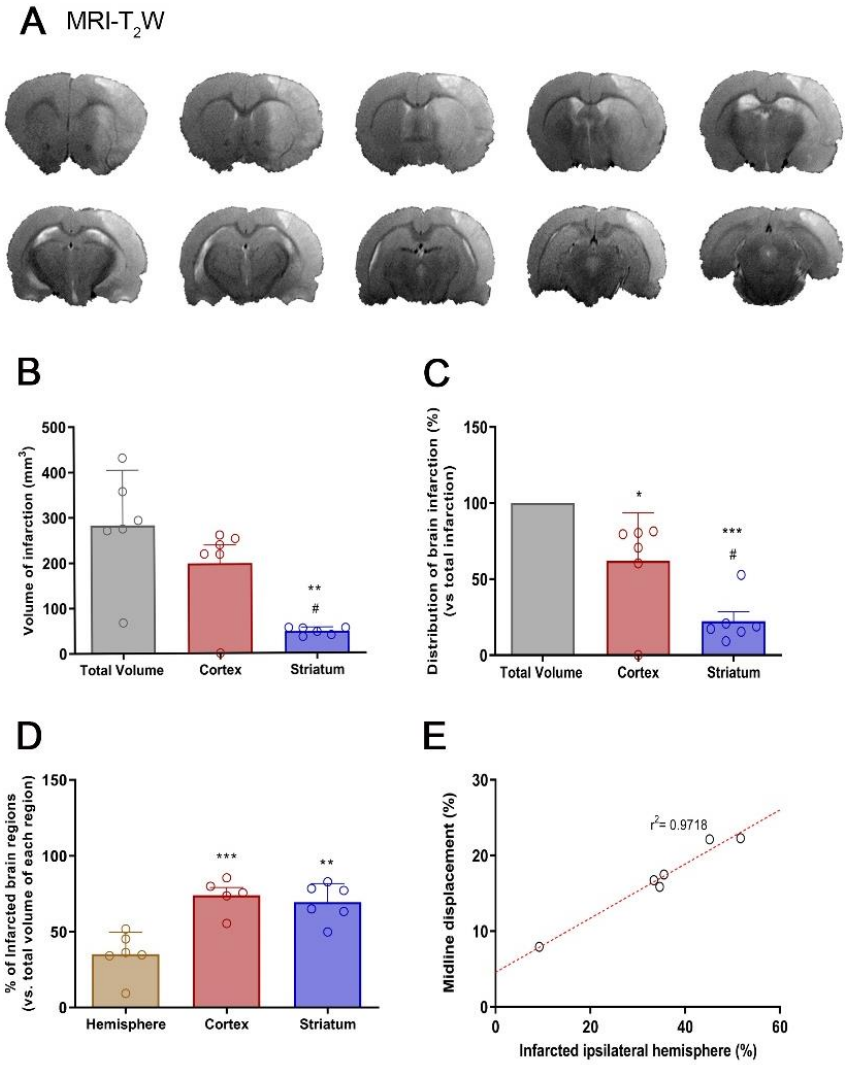

Figure 4. Description of the brain infarction. A: MRI-T_2W images of axial planes at day 1 after cerebral ischemia. B: Total volume of infarction and volumes of infarction in the cortex and striatum (mm^3) (**$p < 0.01$ striatum to total volume; $^{\#}p < 0.05$ striatum to cortex). C: Distribution of infarction in the cortex and striatum (%) (*$p < 0.05$ cortex to total volume and ***$p < 0.001$ striatum to total volume; $^{\#}p < 0.05$ striatum to cortex). D: Percentages of infarcted volume in the hemisphere, cortex and striatum when compared to total volume of each region (%) (**$p < 0.01$ striatum to hemisphere and ***$p < 0.001$ cortex to hemisphere). E: Lineal regression between infarcted ipsilateral hemisphere volume (%) and midline displacement (%) ($r^2 = 0.9718$, $p < 0.001$).

Longitudinal PET imaging of A_2ARs after cerebral ischemia in rats

The longitudinal expression of A_2ARs was evaluated with *in vivo* PET imaging using the radiotracer [^{11}C]SCH442416 before (control) and at the following 28 days after cerebral ischemia. The intensity of the PET signal decreased in the ipsilateral striatum at day 1 after cerebral ischemia when compared to baseline levels (day 0) followed by an increase at day 3 after ischemia. Subsequently, PET signal decreased from days 7 to 28 in relation to day 3 (Fig. 5). In contrast, the contralateral striatum did not show differences along different days after cerebral ischemia.

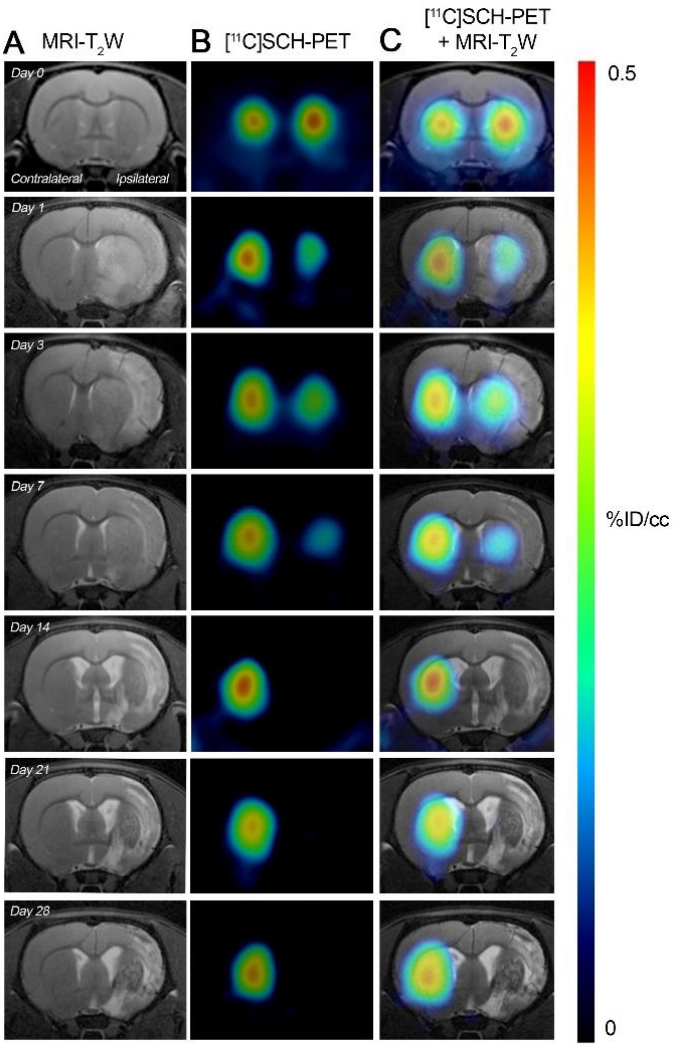

Figure 5. Longitudinal images of MRI and [^{11}C]SCH442416-PET before and after ischemia. MRI-T_2W (A) and [^{11}C]SCH442416-PET (B) images of a representative rat brain before (day 0) and at days 1, 3, 7, 14, 21 and 28 after ischemic stroke. MRI-T_2W (A) and co-registered [^{11}C]SCH442416-PET- MRI-T_2W (B) axial images show the ischemic lesion evolution over one month after stroke onset.

PET imaging quantification of A_2ARs after ischemic stroke in rats

The percentage of injected dose per cubic centimetre (%ID/cc), as well as kinetic parameters in specific brain regions were analysed, including both the striatum and cortex, in control (day 0) and during the following month after ischemic stroke in rats.

In the ipsilateral striatum, PET signal uptake (%ID/cc) showed the highest value at day 3 in comparison to control (day 0) and other time points after ischemia (Fig. 6A). In contrast, the peak value of BPnd was observed at day 0 followed by a decrease at day 1 after the ischemic stroke ($p < 0.01$). Subsequently, BPnd increased at day 3 and declined progressively from day 7 to 28 ($p < 0.05$, $p < 0.01$, $p < 0.001$) (Fig. 6C). Similarly, the highest %ID/cc value was observed at day 3 in relation to control (day 0) and other time points in the contralateral striatum (Fig. 6B). However, non-significant differences of BPnd were observed before and after ischemia (Fig. 6D).

Values of the influx (R_1) and efflux (k_{2a}) at day 0 in the cerebral striatum showed that the concentration of radiotracer that entered to the region was higher than the concentration returned to the blood. No significant differences were observed for R_1 values in both the ipsilateral and contralateral striatum and for values of efflux (k_{2a}) in the ipsilateral striatum. However, values of efflux (k_{2a}) showed a significant decrease at days 7 and 21 in relation to control (day 0) ($p < 0.05$) (Fig. 6E to H).

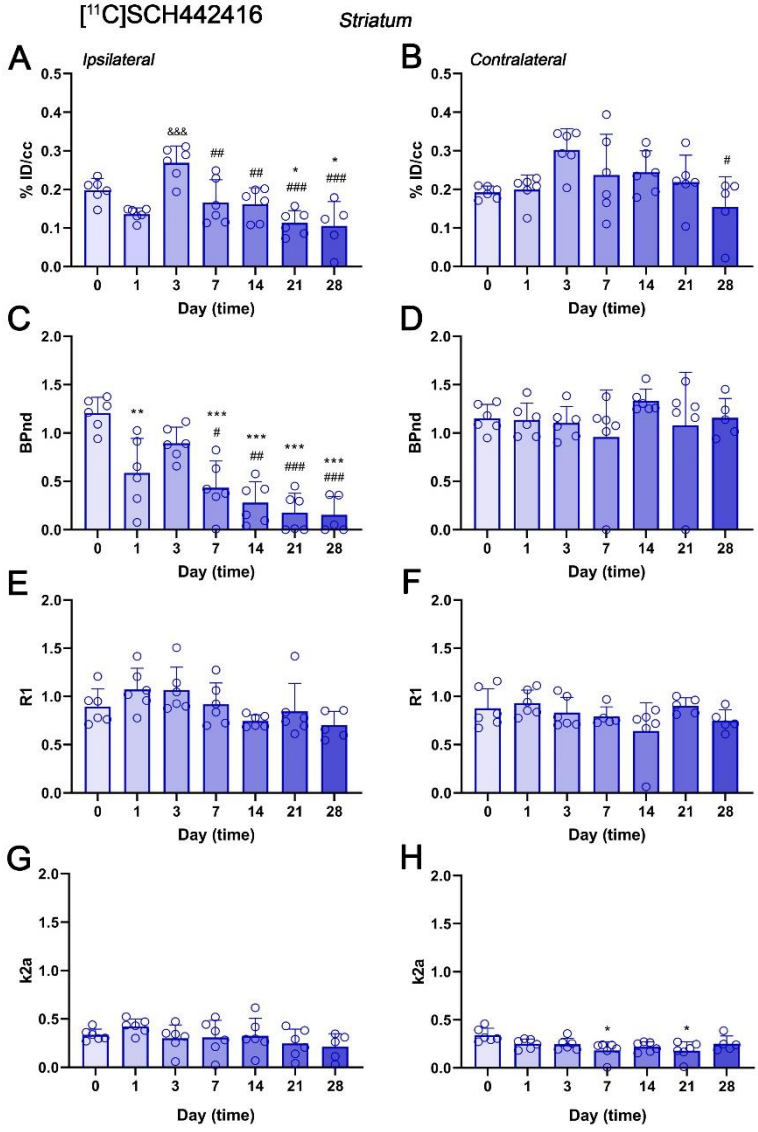

Figure 6. The kinetic parameters of A_2ARs in the striatum. A, B: The percentage of injected dose per cubic centimetre (%ID/cc) in the ipsilateral (A) and the contralateral striatum (B) before (day 0) and the following month (days 1, 3, 7, 14, 21 and 28) of ischemic

stroke. C to H: Kinetic parameters of BPnd, R_1 and k_2a in the ipsilateral and the contralateral striatum obtained by SRTM (*$p < 0.05$, **$p < 0.01$ and ***$p < 0.001$ compared to day 0; $^{\&\&\&}p < 0.001$ compared to day 1; $^{\#}p < 0.05$, $^{\#\#}p < 0.01$ and $^{\#\#\#}p < 0.001$ compared to day 3).

Similarly to the values observed in the striatum (Fig. 6A-B), PET signal uptake (%ID/cc) showed the highest value at day 3 in relation to control (day 0) and other time points after ischemia in both the ipsilateral and contralateral cortex (Fig. 7A-B). However, the cortex before (day 0) and at different days after ischemia showed negligible BPnd values. Despite this, there was a slight but significant increase at day 3 in relation to day 1 ($p < 0.05$), followed by a significant decrease at days 14, 21 and 28 ($p < 0.05$) in the ipsilateral cortex (Fig. 7C).

Contrary to the values observed in the striatum (Fig. 6E to H), values of the radiotracer influx (R_1) and efflux (k_2a) at day 0 were similar in both the ipsilateral and contralateral cortex, which suggested that almost all the radiotracer concentration that entered to the cerebral cortex returned to the bloodstream (Fig. 7E to H).

These results showed similar radiotracer influx values to the cortex before and after ischemia. However, the radiotracer efflux to the blood was impaired after ischemia in comparison to control cerebral cortex (day 0). In addition, BPnd for [^{11}C]SCH44241 showed negligible values before and after ischemia. Therefore, our results suggested that %ID/cc values observed in both the ipsilateral and contralateral cerebral cortex were the result of non-specific binding.

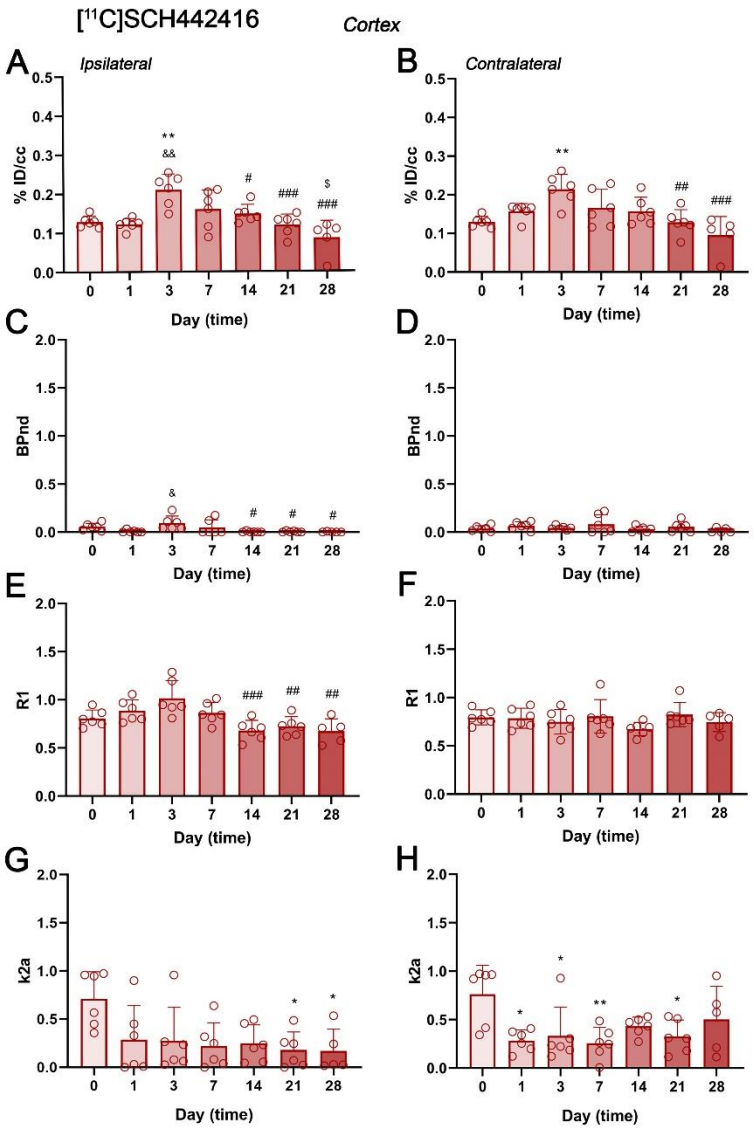

Figure 7. The kinetic parameters of A_2ARs in the cortex. A, B: The percentage of injected dose per cubic centimetre (%ID/cc) in the ipsilateral (A) and the contralateral cortex (B) before (day 0) and the following month (days 1, 3, 7, 14, 21 and 28) of ischemic stroke. C to H: Kinetic parameters of BPnd, R_1 and k_2a in the ipsilateral and the contralateral cortex obtained by SRTM (*$p < 0.05$ and **$p < 0.01$ compared to day 0; $^{\&}p < 0.05$ and $^{\&\&}p < 0.01$ compared to day 1; $^{\#}p < 0.05$, $^{\#\#}p < 0.01$ and $^{\#\#\#}p < 0.001$ compared to day 3; $^{\$}p < 0.05$ compared to day 7).

Discussion

This study showed the *in vivo* distribution of A_2ARs in healthy conditions and after ischemic stroke in rat brains by [^{11}C]SCH442416-PET imaging. In the recent years, adenosine has been described to have a role in response to ischemic stroke (Ganesana & Benton, 2018). Therefore, it has been suggested to be an important pharmacological target in ischemic stroke due to its high concentrations after hypoxic conditions.

Our findings demonstrated that *in vivo* PET imaging was a useful technique for quantifying A_2ARs in healthy and pathological conditions after ischemia. Particularly, our main results showed that A_2ARs expression was mainly restricted to the striatum in healthy conditions (Fig. 3B), in contrast to A_1ARs, which are widely distributed within the entire brain (Joya et al., 2021). Likewise, these results were consistent with

those previously described that showed a high density of A_2ARs in the rat striatum (Rosin et al., 1998). In addition, other studies observed that specific radiotracers for A_2ARs such as [^{11}C]SCH442416 and [^{11}C]Preladenant rapidly accumulated in the brain striatum of rats (Zhou et al., 2014), monkeys (Moresco et al., 2005; Zhou et al., 2017) and humans (Ramlackhansingh et al., 2011; Sakata et al., 2017). Overall, this study evidenced the usefulness of [^{11}C]SCH442416 for studying the *in vivo* distribution of A_2ARs by PET imaging.

The SRTM kinetic model was used to quantify the kinetics of [^{11}C]SCH442416 distribution in both rat striatum and cortex, since those are the most affected areas by model of preclinical stroke used in this study (MCAO) (Fluri et al., 2015). In the healthy striatum (day 0), the influx (R_1) of the radiotracer was higher than its efflux (k_2a) from the target tissue to the bloodstream, which suggested that the radiotracer remained in the striatum. These findings were supported by the increase of BPnd values in the striatum, evidencing the radiotracer binding to A_2ARs. In contrast, healthy rat brain cortex displayed high influx (R_1) and efflux (k_2a) radiotracer values together with negligible BPnd values. Overall, these results showed a higher A_2ARs concentration in the striatum in relation to cerebral cortex in healthy conditions (Fig. 3D-F).

At 1 day after ischemia, [^{11}C]SCH442416-PET uptake (%ID/cc) decreased in the ipsilateral striatum, due to the neuronal loss after hypoxic conditions. However, a slight recovery of the signal was observed at day 3 followed by a sharp decline from day 7 to 28 (Fig. 6A). These results were confirmed by SRTM that showed a BPnd increase at day 3 in relation to day 1 followed by a progressive decline from day 7 to 28. Additionally, the influx (R_1) and the efflux (k_2a) radiotracer values showed non-significant differences along the month following ischemia in both the ipsilateral and contralateral striatum (Fig. 6E to H). Altogether, these findings suggested that the increase of [^{11}C]SCH442416 BPnd observed in the ipsilateral striatum at day 3 after ischemia could be related to a higher expression of A_2ARs.

Within the cerebral cortex, [^{11}C]SCH442416-PET uptake (%ID/cc) increased significantly at day 3 after ischemia in relation to previous days followed by a sharp decrease later on (Fig. 7A-B). Nevertheless, the values obtained by SRTM showed that BPnd barely changed and was negligible before (day 0) and after ischemic stroke (Fig. 7C-D). Furthermore, the influx (R_1) was maintained at similar values before and after ischemia. In contrast, the efflux (k_2a) of the radiotracer was characterised by a sharp decline after ischemia in relation to day 0 in both the ipsilateral and contralateral cortex (Fig. 7E to H). Taken together, these results suggested that %ID/cc values observed in the cerebral cortex can be the result of non-specific binding of [^{11}C]SCH442416. Despite these findings, PET results should be validated by immunohistochemistry of A_2ARs in both the healthy and ischemic brain.

Finally, this study showed that use of kinetic models such as SRTM can provide a more concise quantification of *in vivo* A_2ARs distribution. Indeed, SRTM has been described as an accurate model to analyse the kinetics of a radiotracer when mapping A_2ARs using the cerebellum as the reference tissue (Zhou et al., 2017). However, SRTM assumes that the volume of the radiotracer is equally distributed in both the reference tissue and tissue of interest. As the blood brain barrier (BBB) is usually disrupted after ischemic stroke, the values obtained by SRTM might be influenced. As a result, SRTM would not be an accurate model to study

the brain kinetics of a radiotracer following cerebral ischemia. Despite this, Martin and colleagues showed that the disruption of BBB did not affect the accuracy of SRTM for the evaluation of similar radiotracers to study brain receptors after cerebral ischemia in rats. These authors showed similar [^{11}C]raclopride distribution using both *in vivo* imaging and *ex vivo* autoradiography (Martin et al., 2013). Hence, our *in vivo* PET imaging data should be validated by using *ex vivo* autoradiography to discard BBB disruption effect on [^{11}C]SCH442416 uptake after stroke.

Conclusions

To our knowledge, this was the first study that analysed the expression of A_2ARs by PET in both healthy and ischemic conditions. [^{11}C]SCH442416-PET demonstrated that A_2ARs were mainly expressed in the healthy rat striatum. Additionally, the present findings showed that the expression of A_2ARs increased in the ipsilateral striatum at day 3 after ischemic stroke followed by a progressive decrease later on. Finally, this study confirmed that PET quantification of [^{11}C]SCH442416 using SRTM provided a more accurate information compared to the uptake signal (%ID/cc). Overall, the present study evidenced that [^{11}C]SCH442416-PET imaging was a useful technique for analysing the *in vivo* distribution of A_2ARs in the rat brain. However, further research is needed to gain knowledge about the possible function of A_2ARs after ischemia.

References

Bauer, A., & Ishiwata, K. (2009) Adenosine Receptor Ligands and PET Imaging of the CNS. In C. Wilson & S. Mustafa (Eds.), *Adenosine Receptors in Health and Disease*: *Handbook of Experimental Pharmacology* (pp. 617-642). Berlin, Heidelberg: Springer. https://doi.org/10.1007/978-3-540-89615-9_19

Belov Kirdajova, D., Kriska, J., Tureckova, J., & Anderova, M. (2020). Ischemia-Triggered Glutamate Excitotoxicity From the Perspective of Glial Cells. *Frontiers in Cellular Neuroscience*, *14*. https://doi.org/10.3389/fncel.2020.00051

Borea, P. A., Gessi, S., Merighi, S., Vincenzi, F., & Varani, K. (2018). Pharmacology of Adenosine Receptors: The State of the Art. *Physiological Reviews*, *98*(3), 1591–1625. https://doi.org/10.1152/physrev.00049.2017

Broughton, B. R., Reutens, D. C., & Sobey, C. G. (2009). Apoptotic Mechanisms After Cerebral Ischemia. *Stroke*, *40*(5). https://doi.org/10.1161/strokeaha.108.531632

Burnstock, G. (2007). Purine and pyrimidine receptors. *Cellular and Molecular Life Sciences*, *64*(12), 1471–1483. https://doi.org/10.1007/s00018-007-6497-0

Dirnagl, U., Iadecola, C., & Moskowitz, M. A. (1999). Pathobiology of ischaemic stroke: an integrated view. *Trends in Neurosciences*, *22*(9), 391–397. https://doi.org/10.1016/s0166-2236(99)01401-0

Dunwiddie, T. V., & Masino, S. A. (2001). The Role and Regulation of Adenosine in the Central Nervous System. *Annual Review of Neuroscience*, *24*(1), 31–55. https://doi.org/10.1146/annurev.neuro.24.1.31

Feigin, V. L., Norrving, B., & Mensah, G. A. (2017). Global Burden of Stroke. *Circulation Research*, *120*(3), 439–448. https://doi.org/10.1161/circresaha.116.308413

Fluri, F., Schuhmann, M. K., & Kleinschnitz, C. (2015). Animal models of ischemic stroke and their application in clinical research. *Drug design, development and therapy*, *9*, 3445–3454. https://doi.org/10.2147/DDDT.S56071

Fredholm, B. B., IJzerman, A. P., Jacobson, K. A., Klotz, K. N., & Linden, J. (2001). International Union of Pharmacology. XXV. Nomenclature and classification of adenosine receptors. *Pharmacological reviews*, *53*(4), 527–552.

Ganesana, M., & Venton, B. J. (2018). Early changes in transient adenosine during cerebral ischemia and reperfusion injury. *PloS one*, *13*(5), e0196932. https://doi.org/10.1371/journal.pone.0196932

Grysiewicz, R. A., Thomas, K., & Pandey, D. K. (2008). Epidemiology of Ischemic and Hemorrhagic Stroke: Incidence, Prevalence, Mortality, and Risk Factors. *Neurologic Clinics*, *26*(4), 871–895. https://doi.org/10.1016/j.ncl.2008.07.003

Janssen, B., Vugts, D. J., Funke, U., Molenaar, G. T., Kruijer, P. S., van Berckel, B. N., Lammertsma, A. A., & Windhorst, A. D. (2016). Imaging of neuroinflammation in Alzheimer's disease, multiple sclerosis and stroke: Recent developments in positron emission tomography. *Biochimica et Biophysica Acta*, *1862*(3), 425–441. https://doi.org/10.1016/j.bbadis.2015.11.011

Joya, A., Ardaya, M., Montilla, A., Garbizu, M., Plaza-García, S., Gómez-Vallejo, V., Padro, D., Gutiérrez, J. J., Rios, X., Ramos-Cabrer, P., Cossío, U., Pulagam, K. R., Higuchi, M., Domercq, M., Cavaliere, F., Matute, C., Llop, J., & Martín, A. (2021). In vivo multimodal imaging of adenosine A1 receptors in neuroinflammation after experimental stroke. *Theranostics*, *11*(1), 410–425. https://doi.org/10.7150/thno.51046

Lammertsma, A. A., & Hume, S. P. (1996). Simplified Reference Tissue Model for PET Receptor Studies. *NeuroImage*, *4*(3), 153–158. https://doi.org/10.1006/nimg.1996.0066

Martín, A., Domercq, M., & Matute, C. (2018). Inflammation in stroke: the role of cholinergic, purinergic and glutamatergic signaling. *Therapeutic Advances in Neurological Disorders*, *11*, 175628641877426. https://doi.org/10.1177/1756286418774267

Martín, A., Gómez-Vallejo, V., Sebastián, E. S., Padró, D., Markuerkiaga, I., Llarena, I., & Llop, J. (2013). In Vivo Imaging of Dopaminergic Neurotransmission after Transient Focal Ischemia in Rats. *Journal of Cerebral Blood Flow & Metabolism*, *33*(2), 244–252. https://doi.org/10.1038/jcbfm.2012.162

Moresco, R. M., Todde, S., Belloli, S., Simonelli, P., Panzacchi, A., Rigamonti, M., Galli-Kienle, M., & Fazio, F. (2005). In vivo imaging of adenosine A_2A receptors in rat and primate brain using [11C]SCH442416. *European Journal of Nuclear Medicine and Molecular Imaging*, *32*(4), 405–413. https://doi.org/10.1007/s00259-004-1688-5

Peng, W., Wu, Z., Song, K., Zhang, S., Li, Y., & Xu, M. (2020). Regulation of sleep homeostasis mediator adenosine by basal forebrain glutamatergic neurons. *Science*, *369*(6508), eabb0556. https://doi.org/10.1126/science.abb0556

Ramlackhansingh, A. F., Bose, S. K., Ahmed, I., Turkheimer, F. E., Pavese, N., & Brooks, D. J. (2011). Adenosine 2A receptor availability in dyskinetic and nondyskinetic patients with Parkinson disease. *Neurology*, *76*(21), 1811–1816. https://doi.org/10.1212/wnl.0b013e31821ccce4

Rosin, D. L., Robeva, A., Woodard, R. L., Guyenet, P. G., & Linden, J. (1998). Immunohistochemical localization of adenosine A2A receptors in the rat central nervous system. *The Journal of comparative neurology*, *401*(2), 163–186.

Sakata, M., Ishibashi, K., Imai, M., Wagatsuma, K., Ishii, K., Zhou, X., de Vries, E. F., Elsinga, P. H., Ishiwata, K., & Toyohara, J. (2017). Initial Evaluation of an Adenosine A_2A Receptor Ligand, 11C-Preladenant, in Healthy Human Subjects. *Journal of Nuclear Medicine*, *58*(9), 1464–1470. https://doi.org/10.2967/jnumed.116.188474

Zhou, X., Boellaard, R., Ishiwata, K., Sakata, M., Dierckx, R. A., de Jong, J. R., Nishiyama, S., Ohba, H., Tsukada, H., de Vries, E. F., & Elsinga, P. H. (2017). In Vivo Evaluation of 11C-Preladenant for PET Imaging of Adenosine A_2A Receptors in the Conscious Monkey. *Journal of Nuclear Medicine*, *58*(5), 762–767. https://doi.org/10.2967/jnumed.116.182410

Zhou, X., Khanapur, S., Huizing, A. P., Zijlma, R., Schepers, M., Dierckx, R. A. J. O., van Waarde, A., de Vries, E. F. J., & Elsinga, P. H. (2014). Synthesis and Preclinical Evaluation of 2-(2-Furanyl)-7-[2-[4-[4-(2-[11C]methoxyethoxy)phenyl]-1-piperazinyl]ethyl]7H-pyrazolo[4,3-e][1,2,4]triazolo[1,5-c]pyrimidine-5-amine ([11C]Preladenant) as a PET Tracer for the Imaging of Cerebral Adenosine A_2A Receptors. *Journal of Medicinal Chemistry*, *57*(21), 9204–9210. https://doi.org/10.1021/jm501065t